Catalysis Today 149 (2010) 281–287

Contents lists available at ScienceDirect

Catalysis Today

journal homepage: www.elsevier.com/locate/cattod

Heterogeneous transesterification processes by using CaO supported on zinc oxide as basic catalysts

Ana C. Alba-Rubio [a], José Santamaría-González [a], Josefa M. Mérida-Robles [a], Ramón Moreno-Tost [a], David Martín-Alonso [b], Antonio Jiménez-López [a], Pedro Maireles-Torres [a,*]

[a] Departamento de Química Inorgánica, Cristalografía y Mineralogía (Unidad Asociada al ICP-CSIC), Facultad de Ciencias, Universidad de Málaga, Campus de Teatinos, 29071 Málaga, Spain
[b] Instituto de Catálisis y Petroleoquímica, CSIC, c/ Marie Curie 2, Campus Cantoblanco, 28049 Madrid, Spain

ARTICLE INFO

Article history:
Available online 30 October 2009

Keywords:
Transesterification
Biodiesel
Heterogeneous catalysis
Calcium oxide
Zinc oxide

ABSTRACT

Zinc oxide, obtained by thermal decomposition of zinc oxalate, has been impregnated with different amounts of calcium oxide, and used as solid catalyst for transesterification processes. Catalysts have been characterized by chemical analysis, XRD, XPS, FT-IR, SEM, N_2 adsorption–desorption at 77 K and CO_2-TPD. The catalytic behaviour has been evaluated by choosing two transesterification processes: a simple model such as the reaction between ethyl butyrate and methanol and the production of biodiesel from sunflower oil and methanol. Calcium oxide is stabilized by filling the mesoporous network of ZnO, as reveal the corresponding pore size distributions, thus avoiding the lixiviation of the active phase in the reaction medium. These supported CaO catalysts, thermally activated at 1073 K, can give rise to FAME (fatty acid methyl esters) yield higher than 90%, after 2 h of reaction, when a methanol:oil molar ratio of 12 and 1.3 wt% of the catalyst with a 16 wt% CaO were employed.

1. Introduction

Nowadays, most of fuels are based on raw materials of fossil source, provoking in most of countries an enormous problem of energy dependency and environmental contamination. The exhaustion of the fossil resources, the increase of the polluting emissions and the fact that two third parts of the oil reserves are located in the unstable region of Persian Gulf forces the necessity to find alternatives to fossil fuels.

In this context, biodiesel obtained by transesterification of vegetable oils is a viable alternative to replace petrodiesel, and its use has become more attractive due to the environmental concerns and the renewable energy promotion policies. Biodiesel obtained from the transesterification of renewable vegetable oils, mainly with methanol or ethanol, is a mixture of monoalkyl esters of long chain fatty acids. The biodiesel displays some environmental advantages such as lower emissions of CO, unburned hydrocarbons, particulate matter and SO_2. Homogenous catalysis is normally employed to accomplish this reaction with a high yield of methyl esters. The reaction can be catalyzed by base and acid catalysts or enzymes. The base catalysts include hydroxides and alcoxydes of sodium and potassium [1–10]. The most used acid catalysts are sulphuric, hydrochloric and sulphonic acids [11–13]. It is also feasible the employment of lipases as biocatalysts [14,15]. The transesterification catalyzed by bases is much faster, and it is commercially chosen since they proceed under moderate operating conditions. Moreover, in this homogeneous process, triglycerides and alcohol must be anhydrous since soap formation is favoured by the presence of water [16], thus diminishing the esters yield and making difficult the separation of esters and glycerol. In addition, the free fatty acid content of the oil must be low. In the presence of high water and free fatty acids contents, the transesterification catalyzed by acids is preferred [17]. Most important advances concerning the process of biodiesel production are going to come from the better selection of vegetal species and also from the development of solid catalysts to move toward a heterogeneous catalysis, thus diminishing the number of steps of industrial process. Among the advantages of a heterogeneous catalytic process, it can be mentioned: (1) the easy reusability of the solid catalyst, since the catalyst is not consumed by foam formation, (2) glycerol emulsions in the organic phase are not formed, whose elimination needs time for the separation phases, and (3) biodiesel washing to separate glycerol and catalyst is avoided, saving the consumption and purification of water.

The main drawback of the current solid catalysts is their limited catalytic activity in comparison to the homogeneous process, and, in general, they require more severe experimental conditions to reach vegetable oil conversion similar to that of the homogenous process [18].

* Corresponding author. Tel.: +34 952131873; fax: +34 952137534.
E-mail address: maireles@uma.es (P. Maireles-Torres).

0920-5861/$ – see front matter © 2009 Elsevier B.V. All rights reserved.
doi:10.1016/j.cattod.2009.06.024

Gryglewicz [1] has evaluated the behaviour of a series of catalysts based on alkaline earth metal oxides, hydroxides and methoxydes, for the methyl ester production from rapeseed oil and methanol. This research has demonstrated that the transesterification can be effectively catalyzed by basic compounds derived from alkaline earth metals: CaO, $Ca(OCH_3)_2$ and $Ba(OH)_2$. Recently, López Granados et al. [9] have shown that CaO might be a good option like heterogeneous catalyst since this catalyst reached the maximum conversion of triglycerides within the first 60 min of reaction. Zhu et al. [19] have also used calcium oxide, and they have demonstrated that the basic strength of CaO is sufficient for the transesterification of oil from *Jatropha curcas*. Nevertheless, the addition of agents to eliminate the leached calcium from the catalyst was needed to avoid its presence in biodiesel.

It is evident that an important constraint for the use of these basic materials is the leaching of the active phase in the reaction medium, which would force to introduce additional stages of neutralization and elimination of these species. Under these conditions, the catalytic process operating in the transesterification would be mixed, with contribution of both homogeneous and heterogeneous catalysis, losing the advantages of a purely heterogeneous process for the production of biodiesel. Martín-Alonso et al. [20] have found that potassium supported on γ-Al_2O_3 was leached to the reaction medium strongly diminishing the catalytic activity of the heterogeneous catalyst when it was reused four times, only remaining a residual activity of the solid catalyst. An alternative to stabilize these basic oxides against its leaching is the use of supports that facilitate their dispersion and where the interaction support-active phase could prevent the leaching. Albuquerque et al. [10] have stabilized CaO on a siliceous SBA-15 for the transesterification of sunflower oil with methanol reaching a 95% of triglycerides conversion after 5 h of reaction, without contribution of the homogenous process associated to leached calcium oxide.

On the other hand, zinc oxide is a cheap, stable, re-usable, commercially available and environmentally benign catalyst, used in many catalytic reactions [21]. It is widely used as catalyst support, and it has been demonstrated that the impregnation with alkaline metals originates a good basic solid catalyst for the transesterification of vegetable oils [8]. Zinc oxide was inactive in the transesterification of soybean oil, but when it was impregnated with alkaline nitrates, the activity was greatly enhanced in the case of barium and strontium. However, lixiviation of the active phase was not evaluated.

The aim of this paper is to obtain an active, re-usable catalyst based on calcium oxide supported on ZnO for the transesterification of sunflower oil with methanol using mild reaction conditions. For this purpose, we have prepared a series of catalysts with different CaO loading. These catalysts have been characterized by chemical analysis, XRD, SEM, XPS, FT-IR, CO_2-TPD, and N_2 adsorption–desorption. The transesterification activity has been firstly evaluated using the transesterification of ethyl butyrate with methanol as model reaction, and then the transesterification of sunflower oil with methanol for biodiesel production.

2. Experimental

2.1. Catalysts preparation

Chemicals were supplied by Aldrich, except oxalic acid and ethanol supplied by Normapur–Prolabo, and used as received.

The ZnO support was obtained from zinc oxalate, which was prepared by precipitation after the dropwise addition of a saturated solution of oxalic acid to a saturated zinc acetate aqueous solution, at 313 K, under vigorous stirring for 1 h. The white solid was centrifuged and washed with deionised water and acetone and dried at 353 K. Zinc oxide (ZnO-synt) was obtained after calcination in air of zinc oxalate at 673 K for 90 min (heating rate 2 K min^{-1}). A commercial ZnO (Aldrich) was also used (ZnO-com).

The incorporation of calcium oxide was carried out by impregnation of the ZnO support by means of the incipient wetness method with calcium acetate aqueous solutions. The catalysts (ZnO–*n*CaO, where *n* denotes the CaO loading, varying between 2 and 16 wt%) were prepared after calcination in air at 873 K for 6 h (heating rate 2 K min^{-1}).

2.2. Catalysts characterization

Powder XRD measurements were performed on a Siemens D5000 automated diffractometer, over a 2θ range with Bragg–Brentano geometry using the Cu Kα radiation and a graphite monochromator.

The FT-IR spectra of the samples were recorded as KBr disks in the wavenumber region of 4000–400 cm^{-1} with a Shimadzu model 8300 FT-IR spectrometer.

Scanning electron micrographs (SEM) were obtained on a JEOL SM 840 to observe the morphology of the particles.

X-ray photoelectron spectroscopy (XPS) studies were performed with a Physical Electronics PHI 5700 spectrometer equipped with a hemispherical electron analyzer (model 80-365B) and a Mg Kα (1253.6 eV) X-ray source. High-resolution spectra were recorded at 45° take-off-angle by a concentric hemispherical analyzer operating in the constant pass energy mode at 29.35 eV, using a 720 mm diameter analysis area. Charge referencing was done against adventitious carbon (C 1s 284.8 eV). The pressure in the analysis chamber was kept lower than 5×10^{-6} Pa. PHI ACCESS ESCA-V6.0 F software package was used for data acquisition and analysis. A Shirley-type background was subtracted from the signals. Recorded spectra were always fitted using Gauss–Lorentz curves in order to determine more accurately the binding energy of the different element core levels.

N_2 adsorption–desorption isotherms at 77 K of catalysts calcined at 873 K were obtained using an ASAP 2020 model of gas adsorption analyzer from Micromeritics, Inc. Prior to N_2 adsorption, the samples were evacuated at 473 K and 1×10^{-2} Pa, overnight. Pore size distributions were calculated with the Cranston and Inkley method for cylindrical pores [22].

The basicity of catalysts was studied by temperature-programmed desorption using CO_2 as probe molecule. Catalysts (100 mg) were pretreated under a helium stream at 1073 K for 1 h (20 K min^{-1}, 100 mL min^{-1}). Then, temperature was decreased down to 373 K, and a flow of pure CO_2 (50 mL min^{-1}) was subsequently introduced into the reactor during 1 h. The TPD of CO_2 was carried out between 373 and 1073 K under a helium flow (10 K min^{-1}, 30 mL min^{-1}), and CO_2 was detected by an on-line gas chromatograph (Shimadzu GC-14A) provided with a TCD, after passing by an ice-NaCl trap to eliminate any trace of water.

The elemental analysis was performed on a PERKIN-ELMER 2400 CHN with a LECO VTF900 pyrolysis oven.

2.3. Catalytic activity

The catalytic activity was evaluated in the transesterification of ethyl butyrate (Aldrich) with methanol (ultra pure, Alfa Aesar). The transesterification reaction was performed in a glass bath reactor with a water-cooled condenser, controlled temperature (333 K) and inert atmosphere (N_2). Before the reaction, the catalysts were activated at 1073 K for 1 h (heating rate, 10 K min^{-1}) under a He flow. After cooling, the catalyst was quickly added to the reaction mixture. The reaction was stopped by submerging the reactor in an ice bath. The catalyst was separated by filtration, and the reaction

products were analyzed in a gas chromatograph (Shimadzu GC model 14A) equipped with FID and a capillary silica fused SPB1 column. The analysis of the reaction course was followed by measuring the conversion in each catalytic run from the ethyl butyrate:methyl butyrate areas ratio. The calibration was carried out by representation of 100/conversion (%) as a function of the ethyl butyrate:methyl butyrate areas ratio, thus, minimizing the error in the injection process since this ratio is independent of the injection volume. The most active catalyst was tested in the biodiesel production from sunflower oil, by using a methanol:oil molar ratio of 12, a reaction temperature of 333 K and a catalyst concentration of 1.3 wt%.

The methanolysis of sunflower oil was performed in a three-necked jacketed batch reactor. The experimental procedure has been described elsewhere [9]. Catalysts were previously treated at 1073 K for 1 h, under inert atmosphere. Once the catalyst was at room temperature, 50 g of oil (refined sunflower oil, food grade) was added, and the mixture was heated under strong stirring (1000 rpm) up to 333 K. Then methanol previously heated at 333 K was added to the oil–catalyst mixture by using the dropping funnel. The methanol/oil molar ratio was 12. Aliquots (ca. 2 mL) were taken at different reaction times. The reaction was quenched by addition of an HCl aqueous solution, and the analysis was carried out by following the experimental procedure described elsewhere [9].

In this study the yields to mono and diglycerides were not determined and it is assumed that the FAME yield was close to the triglyceride conversion. This can be considered a good approximation only for conversion larger than 30–40% since it is widely accepted that the selectivity to these products is important for lower triglyceride conversion [2,5,6,23–30]. The content in FAME of the organic layer was determined by following the European regulated procedure EN 14103.

3. Results and discussion

3.1. Catalysts characterization

The elemental analysis of the ZnO–*n*CaO catalysts has evidenced a carbon content lower than 0.4%, indicating that the decomposition of the precursor was successful. The presence of this low percentage of carbon could be attributed to both the thermal decomposition of acetate and the surface carbonation of CaO by atmospheric CO_2.

The XRD patterns of the supports (Fig. 1) show intense peaks at 2θ (°): 31.85, 34.50, 36.34, 47.61 and 56.67, which can be indexed in the hexagonal structure of crystalline ZnO. The ZnO-com is more crystalline than the ZnO-synt, as revealing the more intense diffraction signals. By using the Scherrer equation [31], the size of crystallites of ZnO may be calculated from the XRD patterns, providing average values of 110 nm and 26 nm, for the ZnO-com and ZnO-synt, respectively. These results are expected as a consequence of the synthesis method used for the ZnO-synt support, since the evolved gases from the oxalate decomposition generate lower particle sizes, leading to a lower crystallinity degree. In the XRD patterns of the ZnO–*n*CaO catalysts (Fig. 1), together with the reflections due to ZnO, several signals of cubic CaO and calcite can be observed. Others calcium compounds, such as $Ca(OH)_2$ and $Ca(Zn_2(OH)_6)\cdot 2H_2O$, have not been detected.

The lower crystallinity of ZnO synthesized is confirmed by Scanning Electron Microscopy (Fig. 2). The crystallites of ZnO-com are more homogeneous and larger than those observed for the ZnO-synt, which presents aggregates of variable morphology. The SEM micrographs of the ZnO–*n*CaO catalysts do not reveal the presence of CaO particles segregated from the support, thus pointing to the homogeneous distribution of the active phase on the ZnO. Moreover, as the CaO loading is increased the particles are larger due to the particles sintering.

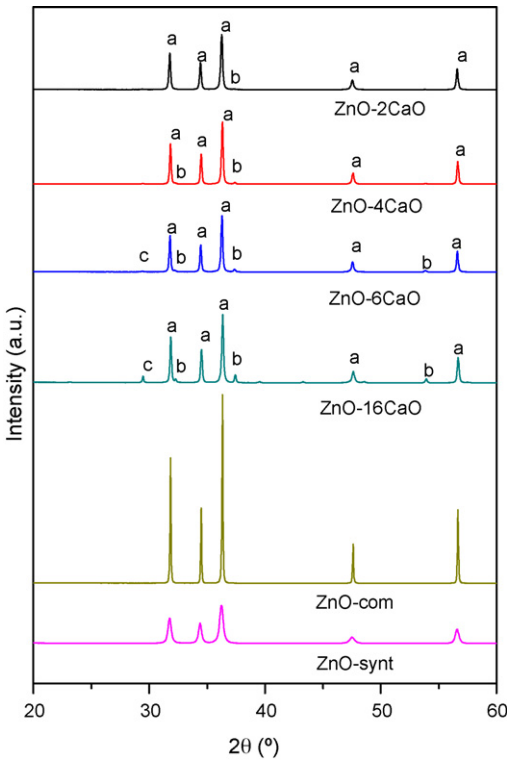

Fig. 1. XRD patterns of ZnO synthesized, ZnO supplied by Aldrich and CaO supported catalysts treated at 873 K: peaks labelled as (a) ZnO (JCPDS file 80-0075), (b) CaO (JCPDS file 77-2376) and (c) calcite–$CaCO_3$ (JCPDS file 86-174).

The textural properties of the two ZnO supports have been evaluated from their N_2 adsorption–desorption isotherms at 77 K (Table 1). The textural parameters corroborate the data deduced from XRD and SEM, since the small crystallites of ZnO-synt gives rise to higher specific surface area, pore volume and average pore diameter. The pore size distribution of ZnO-synt evidences the presence of a large range of pore sizes, mainly located in the mesoporous region, while the ZnO-com only shows micropores (Fig. 3). Nevertheless, in both cases, ZnO is a non-porous solid. The textural parameters of ZnO–*n*CaO catalysts reveal that the incorporation of CaO provokes a noteworthy decrease in the corresponding S_{BET} and pore volume. Moreover, it is noticeably the important decrease of the mesopores contribution, which would indicate that CaO particles are filling this type of pores.

The surface characterization of the ZnO supports and ZnO–*n*CaO catalysts has been carried out by means of XPS. Fig. 4 shows the O 1s, C 1s, Zn 2p and Ca 2p core levels spectra of ZnO–4CaO material as example. The corel level O 1s peak of ZnO and CaO catalysts is asymmetrical, and it can be deconvoluted in two components at 530.1 eV and 531.8 eV which can be assigned to the oxygen in metal oxides (ZnO and CaO) and the oxygen in carbonates, respectively. In the C 1s region, it can be observed two signals at 284.87 eV and 288.64 eV which are ascribed to C–H and carbonate groups, respectively. However, the signal C 1s of carbonate in the CaO catalysts is shifted to higher BE and its intensity is enhanced, indicating that the carbonate is associated to the calcium. The Zn $2p_{3/2}$ signal is symmetrical and appears at 1021.41 eV, which is characteristic of ZnO. Moreover, this signal is not modified by the presence of calcium. The ZnO–*n*CaO catalysts show a well-resolved spin orbit split 2p doublet ($\Delta \sim 3.5$ eV) with $2p_{3/2}$ at 347.5 eV. The core level Ca 2p could be ascribed to Ca^{2+} ions.

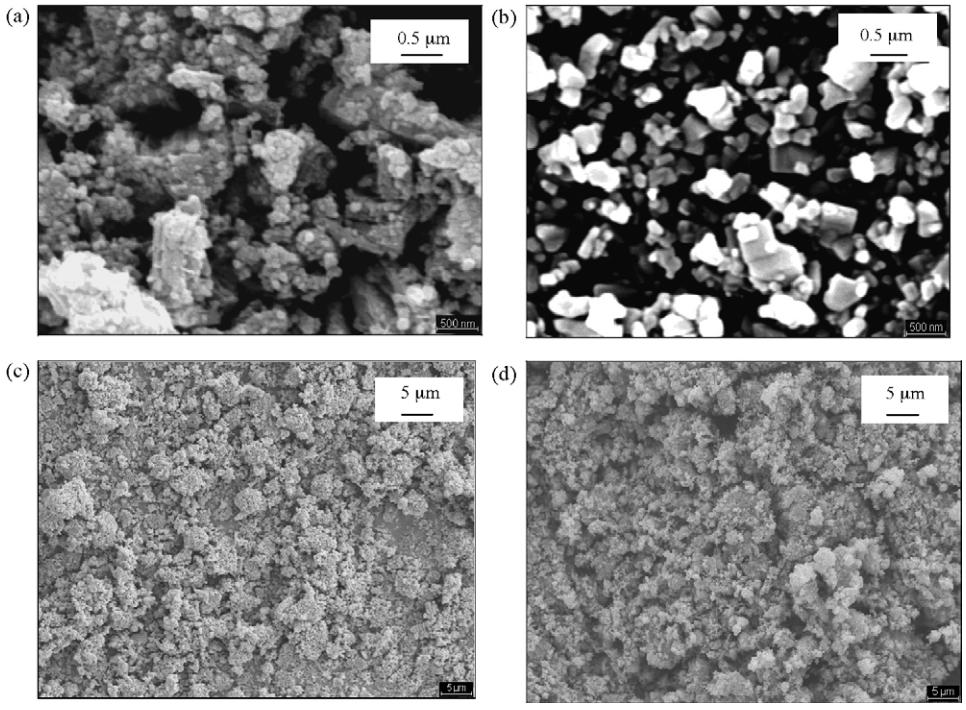

Fig. 2. SEM micrographs of (a) ZnO-synt, (b) ZnO-com, (c) ZnO–2CaO and (d) ZnO–16CaO materials.

The surface chemical compositions determined by XPS are compiled in Table 2. The homogeneity of the CaO distribution on the ZnO support has been proven by choosing three different areas of analysis for two catalysts (ZnO–2CaO and ZnO–6CaO). The results reveal that the active phase is homogeneously dispersed on the surface of the support. Moreover, the Zn/Ca atomic ratio is lower than the theoretical values except for the CaO catalyst with a 2 wt% loading. This fact points out the CaO is located on the surface, thus masking the signal of the ZnO support.

The presence of carbonates has been also confirmed by FT-IR spectroscopy (Fig. 5). The spectra are similar, regardless of the CaO loading, showing bands corresponding to the carbonates species at 875 and 1420 cm^{-1}. It is also detected that the presence of physisorbed water gives rise to the band at 1640 cm^{-1}, bending mode of the O–H bond, and the wide band at 3470 cm^{-1} ascribed to the stretching O–H mode. This band could include the stretching O–H mode of calcium hydroxide [9,21]. The intense bands at wavenumbers below 600 cm^{-1} can be assigned to the vibration modes of ZnO and CaO.

The basicity has been studied by CO_2 temperature-programmed desorption (Fig. 6). The catalysts exhibit two desorption bands, a first one extending between 423 and 623 K and other more intense and well defined centred at 773–873 K. The former could be ascribed to CO_2 desorbed from the ZnO support and the latter to those CO_2 molecules stem from CaO. The fact that the ZnO support does not adsorb CO_2 would point to the existence of a synergy between ZnO and CaO, enhancing the basic character of ZnO. Therefore, catalysts have weak basic sites on the support surface and strong basic sites on the CaO surface, since evolution of CO_2 from calcium carbonates takes place at higher temperatures.

Table 1
Textural properties of ZnO synthesized, ZnO supplied by Aldrich and ZnO–*n*CaO catalysts treated at 873 K.

Catalyst	S_{BET} ($m^2 g^{-1}$)	V_p ($cm^3 g^{-1}$)	$d_{p\ average}$ (nm)
ZnO-com	6.2	0.015	8.1
ZnO-synt	24.1	0.162	23.5
ZnO–2CaO	9.6	0.052	30.6
ZnO–4CaO	7.3	0.029	29.4
ZnO–6CaO	7.5	0.028	15.5
ZnO–16CaO	8.1	0.030	12.4

3.2. Catalytic activity

The catalytic activity of this series of catalysts has been firstly tested in the transesterification of ethyl butyrate with methanol as model reaction. Parameters such as activation temperature, CaO loading, nature of support, time of reaction, lixiviation of active phase, have been studied to achieve the maximum catalytic activity.

The activation temperature has been optimized by treating the ZnO–4CaO catalyst in a flow of helium for an hour at different temperatures, and then avoiding any presence of air in the atmosphere of the reactor. The temperature was varied between

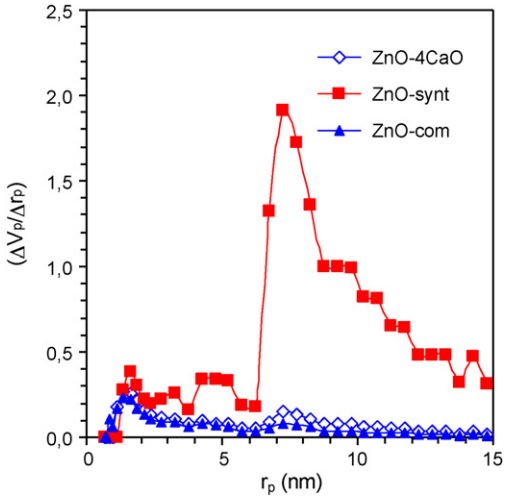

Fig. 3. Cranston and Inkley distribution of pores of ZnO synthesized, ZnO supplied by Aldrich and ZnO–*n*CaO catalysts.

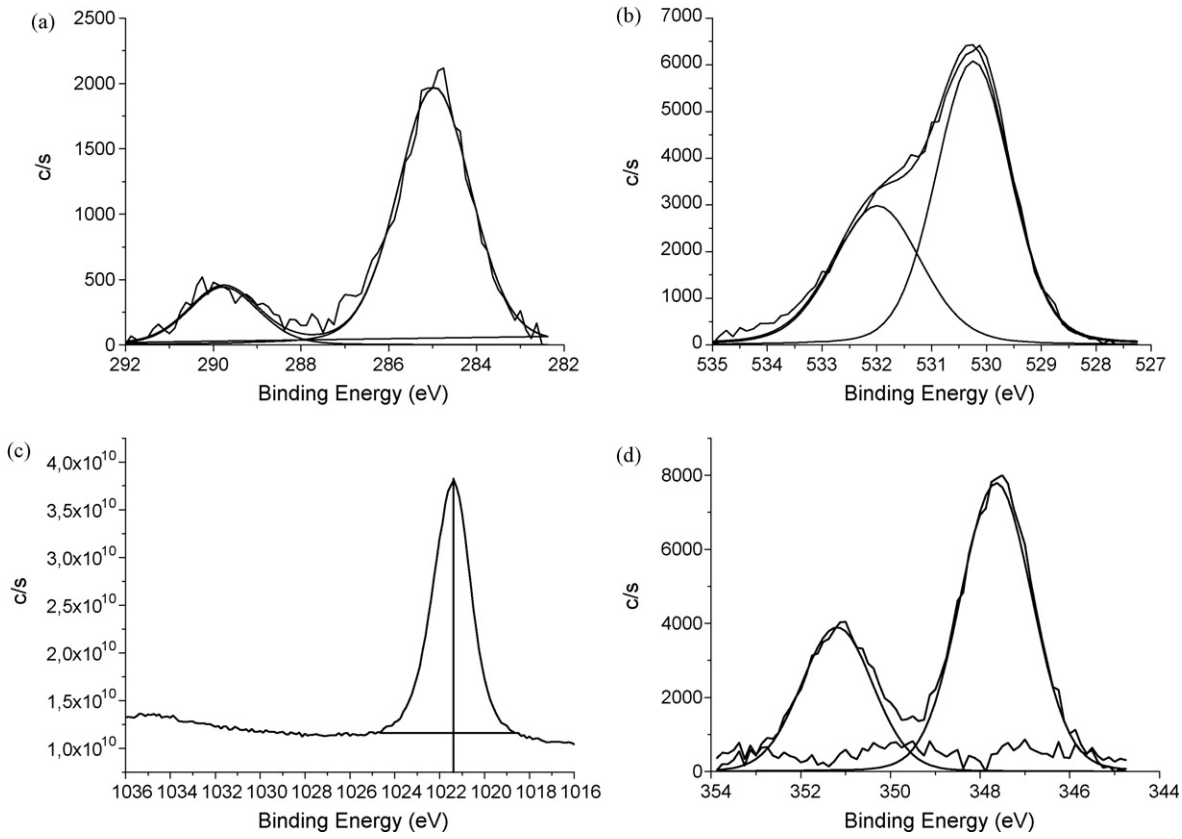

Fig. 4. O 1s, C 1s, Zn 2p and Ca 2p core levels spectra of ZnO–4CaO material: (a) C 1s, (b) O 1s, (c) Zn 2p and (d) Ca 2p.

873 and 1173 K. The ethyl butyrate conversion values show that the optimum temperature was 1073 K (Fig. 7). In the same figure, the catalytic activity as a function of the CaO loading at 1073 K is also displayed. This study reveals that an increment of CaO above 4 wt% does not lead to a better catalytic performance, but rather the conversion of ethyl butyrate decreases up to 35%. This decrease of catalytic activity with the CaO loading may results from the formation of large crystallites of CaO, as demonstrated by the SEM micrographs. Taking into account these results, the influence of the rest of parameters has been studied with the ZnO–4CaO catalyst. The ZnO support did not show catalytic activity in this reaction in spite of its acid–base character.

It has been also evaluated the influence of the structural and textural properties of ZnO used as support, by comparing a commercial ZnO with a synthesized ZnO support. Thus, the conversion of ethyl butyrate using CaO (4 wt%) supported on commercial ZnO was of 28.2%, in contrast with an analogous catalyst prepared with the synthesized ZnO, which reached an ethyl butyrate conversion of 41.2%. This difference may be accounted for the better textural properties and lower crystallite sizes of synthesized ZnO, thus improving the dispersion of the active phase.

Another key parameter to be optimized, mainly for industrial purposes, is the reaction time. Fig. 8 exhibits the evolution of ethyl butyrate conversion until 3 h of reaction on the ZnO–4CaO catalyst activated at 1073 K. The conversion is considerably increased within the first hour, and after 3 h a maximum value of 35% is reached.

Table 2
Binding energies and surface chemical composition, as determined by XPS.

	BE (eV)				Surface atomic ratio		
	Zn $2p_{3/2}$	Ca 2p	O 1s	C 1s	Zn/Ca exp		Zn/Ca theor.
ZnO-synt	1021.4	–	530.1 531.8	284.9 288.6	–	–	–
ZnO–2CaO	1021.4	347.4 350.8	530.1 531.7	285.0 289.6	51.09 37.34 44.05	Average 44.16	33.72
ZnO–4CaO	1021.3	347.6 351.0	530.1 531.8	284.9 289.7	13.93		16.52
ZnO–6CaO	1021.2	347.5 351.0	530.0 531.9	284.9 290.1	7.38 6.77 6.37	Average 6.84	10.78
ZnO–16CaO	1021.6	347.7 351.1	530.8 532.8	285.0 290.0	0.70		3.61

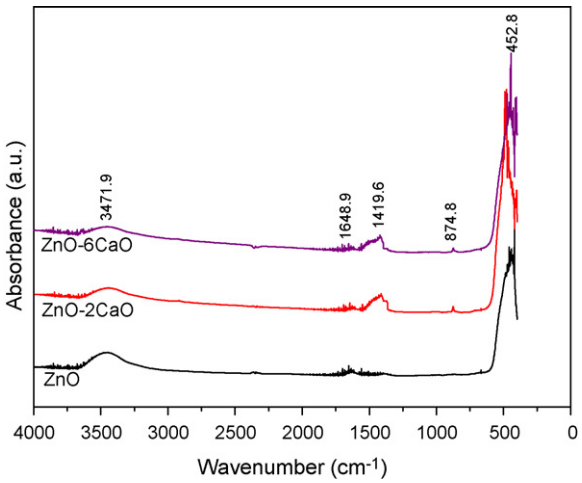

Fig. 5. FT-IR of the ZnO–*n*CaO catalysts and ZnO synthesized.

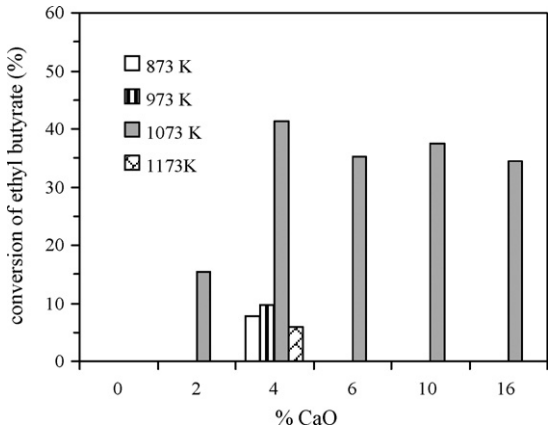

Fig. 7. Catalytic activity of ZnO–*n*CaO catalysts in the transesterification of ethyl butyrate with methanol as a function of the CaO loading and the activation temperature (ZnO–4CaO).

It has been previously stated that the lixiviation of active phase in the reaction medium has to be evaluated for the transesterification of triglycerides since the existence of ions coming from the catalyst in the biodiesel would involve stages of washing and purification of biodiesel, thus losing one of the most important advantages of a heterogeneous process against a homogeneous one. Previous studies have demonstrated that bulk CaO is partially dissolved in the methanolic solution [9,10], and the main goal of this work is to stabilize the calcium oxide to avoid it. The experimental procedure consists in putting the catalyst in contact with methanol at 333 K for 1 h under the same experimental conditions used in the transesterification reaction. Then, the catalyst is filtered and the methanolic solution is mixed with ethyl butyrate carrying out the transesterification reaction for 1 h without catalyst. The conversion values obtained reveal that the lixiviation of active phase is negligible since no conversion of ethyl butyrate is observed. The absence of lixiviation could be supported by the fact that bulk CaO under the same experimental conditions gives rise to a conversion of 8.4%. Therefore, it can be concluded that ZnO used as support is able to stabilize CaO preventing its lixiviation to the reaction medium. This could be explained by the incorporation of CaO particles into the pores, as pointed the lost of the mesoporosity of the support after the incorporation of the active phase.

Finally, these catalysts have been tested in the transesterification of sunflower oil with methanol for biodiesel production. The experimental conditions were: 500 mg of catalyst, activation temperature of 1073 K, stirring rate of 1000 rpm, reaction temperature of 333 K and methanol:oil molar ratio of 12:1. The catalytic behaviour is compared in Fig. 9 with that of 100 mg of CaO produced from decomposition of calcium carbonate at 973 K. After 90 min of reaction, the catalyst with 16 wt% of CaO reached a biodiesel yield as high as bulk CaO. However, the advantage of ZnO–*n*CaO catalysts *versus* CaO is the absence of lixiviation of the active phase, and consequently the contribution of the homogeneous process can be ruled out. Moreover, it is shown that the yield of biodiesel is increased with the CaO loading. While the ZnO–4CaO, after 3 h, shows a biodiesel yield close to 40%, the ZnO–16CaO reaches 90% of triglycerides conversion.

Recently, Ngamcharussrivichai et al. [32] have reported the transesterification of palm kernel oil with methanol using a Ca and Zn mixed oxides prepared by the co-precipitation method. These authors claimed triglycerides conversion of 95% after 3 h of reaction with a catalyst loading of 2 wt% respect of oil content. If

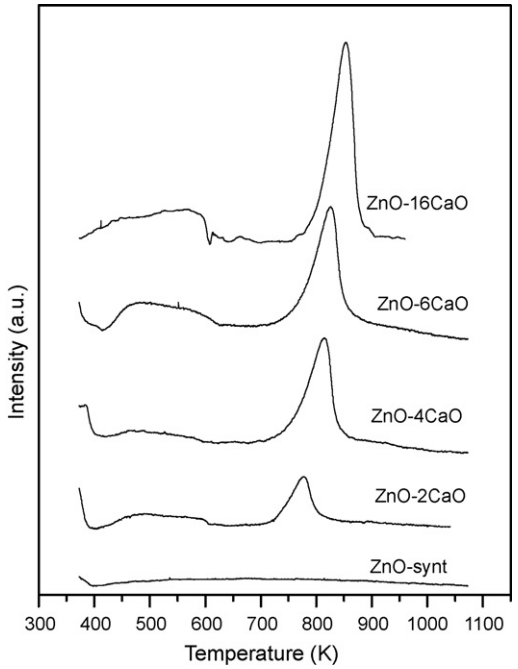

Fig. 6. CO_2-TPD of ZnO-synt and ZnO–*n*CaO catalysts.

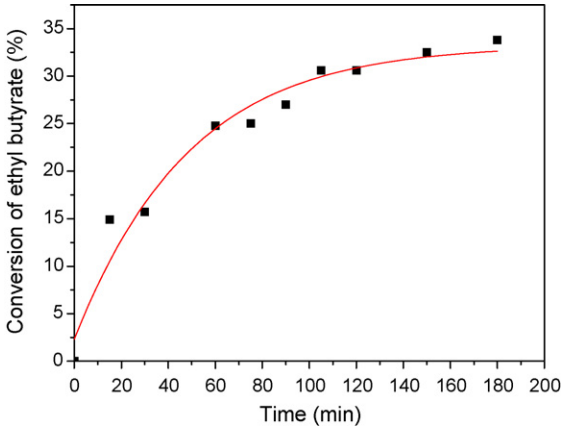

Fig. 8. Catalytic activity of ZnO–4CaO in the transesterification of ethyl butyrate with methanol as a function of the reaction time.

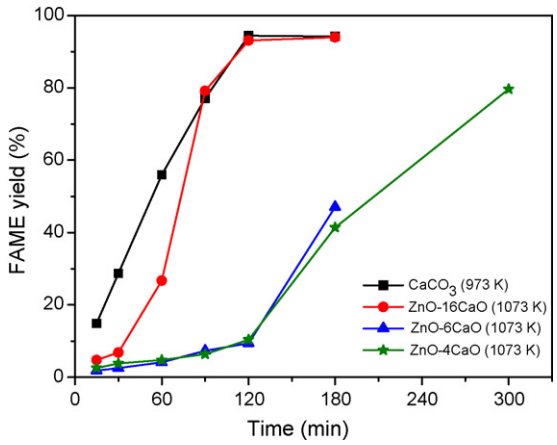

Fig. 9. Yield to FAME obtained by catalytic reaction with catalysts with different CaO loading.

the catalyst loading was increased up to 10 wt%, the yield of biodiesel reached 90% after 30 min of reaction. However, in the present work, a FAME yield higher than 90% has been obtained by using 1.3 wt% of the ZnO–16CaO catalyst, after 2 h of reaction, with a methanol:oil molar ratio of 12. Therefore, it is evident that the preparation method of the ZnO–CaO catalysts has an important influence on the physico-chemical characteristics of the resulting catalysts, and hence on their catalytic performance in transesterification processes.

4. Conclusions

ZnO–*n*CaO catalysts, thermally activated at 1073 K, are active in the transesterification reaction of ethyl butyrate with methanol. These supported CaO catalysts, thermally activated at 1073 K, can give rise to biodiesel yields higher than 90%, after 2 h of reaction, when a methanol:oil molar ratio of 12 and 1.3 wt% of the catalyst with a 16 wt% CaO were employed. Calcium oxide seems to be stabilized by filling the mesoporous of ZnO, thus avoiding the lixiviation of the active phase in the reaction medium.

Acknowledgements

The authors are grateful to financial support from the Spanish Ministry of Education and Science (ENE2006-15116-C04-02 project) and Junta de Andalucía (PO6-FQM-01661). A.C.A.R. and D.M.A. thank the Spanish Ministry of Education and Science and Regional Government of Madrid, respectively, for their predoctoral fellowships.

References

[1] S. Gryglewicz, Bioresour. Technol. 70 (1999) 249–253.
[2] H.J. Kim, B.S. Kang, M.J. Kim, Y.M. Park, D.K. Kim, J.S. Lee, K.Y. Lee, Catal. Today 93–95 (2004) 315–320.
[3] M. Di Serio, M. Ledda, M. Cozzolino, G. Minutillo, R. Tesser, E. Santacesaria, Ind. Eng. Chem. Res. 45 (2006) 3009–3014.
[4] W. Xie, H. Li, J. Mol. Catal. A 255 (2006) 1–9.
[5] D.G. Cantrell, L.J. Gillie, A.F. Lee, K. Wilson, Appl. Catal. A 287 (2005) 183–190.
[6] W. Xie, H. Peng, L. Chen, J. Mol. Catal. A 246 (2006) 24–32.
[7] W. Xie, X. Huang, H. Li, Bioresour. Technol. 98 (2007) 936–939.
[8] Z. Yang, W. Xie, Fuel Process. Technol. 88 (2007) 631–638.
[9] M. López Granados, M.D. Zafra Poves, D. Martín Alonso, R. Mariscal, F. Cabello Galisteo, R. Moreno-Tost, J. Santamaría, J.L.G. Fierro, Appl. Catal. B 73 (2007) 317–326.
[10] M.C.G. Albuquerque, I. Jiménez-Urbistondo, J. Santamaría-González, J.M. Mérida-Robles, R. Moreno-Tost, E. Rodríguez-Castellón, A. Jiménez-López, D.C.S. Azevedo, C.L. Cavalcante Jr., P. Maireles-Torres, Appl. Catal. A 334 (2008) 35–43.
[11] E. Lotero, Y. Liu, D.E. Lopez, K. Suwannakarn, D.A. Bruce, J.G. Goodwin Jr., Ind. Eng. Chem. Res. 44 (2005) 5353–5363.
[12] M. Di Serio, M. Cozzolino, R. Tesser, P. Patrono, F. Pinzari, B. Bonelli, E. Santacesaria, Appl. Catal. A 320 (2007) 1–7.
[13] S. Furuta, H. Matsuhashi, K. Arata, Catal. Commun. 5 (2004) 721–723.
[14] H. Fukuda, A. Kondo, H. Noda, J. Biosci. Bioeng. 92 (2001) 405–416.
[15] M.K. Modi, J.R.C. Reddy, B.V.S.K. Rao, R.B.N. Prasad, Bioresour. Technol. 98 (2007) 1260–1264.
[16] H.J. Wright, J.B. Segur, H.V. Clark, S.K. Coburn, E.E. Langdon, R.N. DuPuis, Oil Soap 21 (1944) 145–148.
[17] G.I. Keim, US Patent 2383601 (1945).
[18] R.G. Bray, Biodiesel Production, SRI Consulting, 2004.
[19] H. Zhu, Z. Wu, Y. Chen, P. Zhang, S. Duan, X. Liu, Z. Mao, Chin. J. Catal. 27 (2006) 391–396.
[20] D. Martín-Alonso, R. Mariscal, R. Moreno-Tost, M.D. Zafra-Poves, M. López Granados, Catal. Commun. 8 (2007) 2074–2080.
[21] F. Tamaddon, M.A. Amrollahi, L. Sharafat, Tetrahedron Lett. 46 (2005) 7841–7844.
[22] R.W. Cranston, F.A. Inkley, Adv. Catal. 9 (1957) 143–154.
[23] J. Van Gerpen, Fuel Process. Technol. 86 (2005) 1097–1107.
[24] Y. Zhang, M.A. Dube, D.D. McLean, M. Kates, Bioresour. Technol. 90 (2003) 229–240.
[25] Y. Zhang, M.A. Dube, D.D. McLean, M. Kates, Bioresour. Technol. 89 (2003) 1–16.
[26] G.J. Suppes, M.A. Dasari, E.J. Doskocil, P.J. Mankidy, M.J. Goff, Appl. Catal. A: Gen. 257 (2004) 213–223.
[27] T. Ebiura, T. Echizen, A. Ishikawa, K. Murai, T. Baba, Appl. Catal. A: Gen. 283 (2005) 111–116.
[28] G.J. Suppes, K. Bockwinkel, S. Lucas, J.B. Botts, M.H. Mason, J.A. Heppert, J. Am. Oil Chem. Soc. 78 (2001) 139–145.
[29] U. Schuchardt, R.M. Vargas, G. Gerbard, J. Mol. Catal. A: Chem. 109 (1996) 37–44.
[30] R. Serchelli, R.M. Vargas, U. Schuchardt, J. Am. Oil Chem. Soc. 76 (1999) 1207–1210.
[31] P. Scherrer, Nachr. Ges. Wiss. Gottingen (1918) 96.
[32] C. Ngamcharussrivichai, P. Totarat, K. Bunyakiat, Appl. Catal. A 341 (2008) 77–85.